International Journal of Bioorganic Chemistry
2017; 2(3): 94-101
http://www.sciencepublishinggroup.com/j/ijbc
doi: 10.11648/j.ijbc.20170203.13

Thermo - Acoustic Approach for Neuron Signals and New Hypothesis for Anesthetics Mechanisms

Svetlana Amirova[1], Tamara Tulaykova[2]

[1]Individual Researcher, Greenville, North Carolina, USA

[2]Moscow Institute of Physics and Technology, Department of Molecular and Chemical Physics, Dolgoprudny, Moscow Region, Russia

Email address:

amirova.svetlana@yahoo.com (S. Amirova), tulaikova@gmail.com (T. Tulaykova)

To cite this article:

Svetlana Amirova, Tamara Tulaykova. Thermo - Acoustic Approach for Neuron Signals and New Hypothesis for Anesthetics Mechanisms. *International Journal of Bioorganic Chemistry*. Vol. 2, No. 3, 2017, pp. 94-101. doi: 10.11648/j.ijbc.20170203.13

Received: February 3, 2017; **Accepted**: February 25, 2017; **Published**: March 30, 2017

Abstract: We consider axon as a cylinder that has acoustic waveguide regimes to concentrate the propagated signals with appropriate deformation of membrane areas. The highest temperature results near the cylinder axis that can cause low-frequency (0.1 - 10 kHz) longitudinal vibrations of axon due to thermal expansion of material. These frequency shifts are very sensitive to the changes in surrounding viscosity, calculations are presented. The same resonance frequencies of both parts of neuron (axon and Soma) were calculated based on structures sizes, but anaesthesia effect could be explained by different frequency changes for both neuron parts to anesthetics admixture in surrounding.

Keywords: Neuron, Acoustics, Vibrations, Mathematics, Anesthetics

1. Introduction

The processes in neurons are interested to study by different approaches and in particular by applying mathematics and engineering methods to find some features and analogy. The voltage clamp technique enabled Huxley and Hodgkin to characterize the electrical response of the giant squid axon to perturbations in voltage. Model Hodgkin - Huxley is a mathematical description by differential equations of the biophysical processes in the cell membrane [1, 2]. They assumed, as it is now customary in the field, that the lipid membrane acts as a simple constant capacitor and that the observed nonlinear currents are due to protein ion-channels which are embedded in an otherwise inert membrane. Subsequent numerous studies of the dynamics of currents in the membranes of nerve cells have provided a lot of interesting data [3-10], etc. It is found that the energy released during discharge of the capacitor membrane over the whole length of the nerve. In particular, the following data were obtained to be used as follows:

- typical temperature change in the membrane $\Delta T \approx 80\mu K$ [4];
- heating of the membrane with account maxim of the current is $E_{max} \approx 200$ μ cal/g = 837.36 μJ/g [4].

The lateral sound velocity was used from data from [4] as $C^2 = 1/(\rho^A K^A)$. There are numerals $7 \cdot 10^3$ m^2/s^2 and $37 \cdot 10^3$ m^2/s^2 for melted and no melted membrane correspondingly. For our calculating we use maximal of these values that give a sound velocity $C \approx 192$ m/s, so we expect that such value is suitable for the entire axon body.

The density $\rho = 1.05$ g/cm^3, specific heat capacity values $C_p = 3768$ J/(kg K) and thermal diffusivity of material $\chi \approx 10^{-7}$ m^2/s were used for further estimations of neuron materials, that is similar to muscle tissue [11].

The possible ways of spread for the energy inside the axon after membrane capacitor discharge were analyzed through thermal, acoustic and deformation processes in the axon and neuron. The energy balance and other basic characteristics of possible physical processes are calculated to prove their possibility to appear. A thin membrane (shell) surrounds the axon (cylinder), so the energy in the shell extends to the center of the cylinder and heats around environment. Well-developed acoustic approaches allowed to assume the sequence of further developments outlined here, build their logical interrelationship and possible greater role. The main hypotheses and physical processes that are offered and investigated in this article, as following:

Thermo - deformation perturbation on the cylindrical shell of the axon results the sound, which is distributed in axon-cylinder as in acoustical waveguide. Axon, which is a cylinder (radius $r = 1$- 20 μm [12]) with the length $L \approx 1 - 10$

mm should have a waveguide regimes for concentrations of the propagated signals. The main (fundamental) sound mode is analyzed here below, because it has the lowest energy level for excitation. As a result, the waveguide provides a sound wave to deform of the adjacent portions from initial terminal to the nerve cell body (soma). Therefore, in the opposite direction tapering toward the axon terminal such wave can not propagate, but it's radiated.

The energy arises during discharge of the capacitor membrane in whole length of axon, this process has about 10^{-3} seconds [1-4]. The calculation here shows that this time $t \approx 10^{-3}$ sec corresponds exactly to nerve cross-section heating time to the full neuron radius $r = a = 10$ μm, there is the next simple estimation:

$$a \approx \sqrt{\chi t} \ , \ t \approx a^2 / \chi \tag{1}$$

The membrane heat concentrates on the cylinder axis, these our calculations are based on common thermal models [13, 14] in technique. Appropriate thermal expansion could cause the generation of longitudinal low-frequency vibrations that are known as reducing of nerves in practice. The amplitudes and frequencies of these oscillations are calculated here exactly on the basis of classical mechanics [15]. The frequency changes for longitudinal vibrations are very sensitive to changes of viscosity in the surrounding liquid [16, 17]. Presented low-frequency vibration approach could explain the effect of anaesthesia in medical practice we suppose; physically it is the change in composition of the surrounding liquid with appropriate changes of density and viscosity. Axon was considered having cylindrical beam profile, but it is attached to ball's head (the neuron centre, Soma) with other ball diameter, R. We supposed that initially the nature grow each pair of axon with Soma, their resonance frequencies for vibrations are equal to each other. In our model of anaesthesia, the small change of viscosity in environment can be the reason for distortion in neuron signal transfer. The viscosity change causes different shifts of values for resonance frequency for the Soma (that is ball) and axon (cylinder). The calculations below confirm the possibility and viability of such hypothesis.

2. Methods for Analyses

The waveguide approach inside axon

Let's consider the axon (at Figure 1a) as a cylindrical waveguide on the basis of the waveguide approach for acoustic signals [18]. Cylindrical waveguide constructed by the boundaries that separate the neurons from the environment, so the waveguide approach for the consideration of acoustic processes is possible. There are calculations for two simples acoustical modes in waveguide structure at Figure 1b. Firstly, the boundary condition on an absolutely rigid wall corresponds to the complete reflection of the signal from the pipe wall, as followed:

$$\frac{\partial}{\partial r} J_m\left(k_r r\right)\big|_{r=a} = k_r J_m{}'\left(k_r a\right) = 0 \tag{2}$$

The cylinder radius at the waveguide cylindrical side is $r = a$; k is a wavenumber and k_r is its radial component; so $k^2 = k_r^2 + k_z^2$. The solution of (2) corresponds to the values of zero for the derivative of the Bessel function $J_0(k_r r)$ and appropriate argument $k_r r = \gamma$ can have values: $\gamma_{00} = 0$, $\gamma_{01} = 3.83$, $\gamma_{02} = 7.02$, $\gamma_{10} = 1.84$, $\gamma_{11} = 5.33$, $\gamma_{12} = 8.54$… The frequency of the lower mode is considered here due to its most likely excited in such acoustic waveguide, it has $\gamma_{mv}=\gamma_{10} = 1.84$. The m, v are the radial and azimuthally numbers for Bessel functions to describe the acoustic distribution for different waveguide modes. This frequency of waveguide mode is:

$$\begin{aligned} &f_{mv} = \frac{\gamma_{mv} C}{2\pi a}, \ \ f_{10} = 0.293C / a \ \ ,... \\ &\gamma_{01} = 3.83, \ \ \gamma_{10} = 1.84, \ \ \gamma_{11} = 5.33... \end{aligned} \tag{3}$$

The low-mode frequencies of mentioned waveguide are: f = 5.6 MHz, 11.7 MHz, 16.3 MHz, with account of sound velocity C = 192 m/s and one example typical axon radius $r = a = 10$μm.

Another option corresponds to the case of a cylindrical waveguide with absolutely soft acoustic walls. The boundary condition at the wall is as follow:

$$J_m\left(k_r r\right)\big|_{r=a} = J_m\left(\gamma_{mv}\right) = 0 \tag{4}$$

The lowest waveguide mode in this case is determined by zero for the transverse component of the field at the cylinder wall, which gives the argument $\gamma_{mv}=\gamma_{00} \approx 2.41$ with its frequency f = 7.4 MHz from equation:

$$\begin{aligned} &f_{00} = \frac{\gamma_{00} C}{2\pi a} = \frac{2.41C}{2\pi a} \\ &\gamma_{00} \approx 2.41 \end{aligned} \tag{5}$$

The penetration depth, h_1, of the high frequency waveguide signal from the side-located source in the longitudinal and transverse directions is estimated through the wave time period $t_1 = 1/f \approx 10^{-7}$ s, as follows:

$$h_1 \approx \sqrt{\chi t_1} \approx 10^{-7} m = 100 \ \ nm \tag{6}$$

The membrane thickness is $h \approx 10$ nm [4], but the result thickness $h_1 \approx 100$ nm from (6) was used as the thermal source of axon heating. Waveguide approach provides fast sound wave propagation to deform of the adjacent portions from the far terminal to the center. In tapered axon's end the lowest acoustic wave can not run due to its radiations on tapering waveguide according to (5) or (3). The lowest waveguide mode needs minimal energy for its excitation, so it will appear with high probability. Energy distribution and its value for each propagated acoustical mode can be calculated using standard methods [18].

Let's consider the heating of the cylindrical axon (marked

2 in Figure 1b) by its cylindrical heated surface (3 in Figure 1b). The Young's modulus equation with cross sectional area, *S*, gives the acted force:

$$F(T,r) = C^2 \rho \alpha T(r) S \quad , E = F / [\alpha T(r) S] = C^2 \rho \tag{7}$$

Then force acts inside membrane along heated cylinder surface *S*, it gives the longitudinal component of the force:

$$F(a,0) = C^2 \rho \alpha T(r) 2\pi \left| (a+h_1)^2 - a^2 \right| \approx 4\pi \alpha \rho C^2 T(a) h_1 a \tag{8}$$

The estimation is for typical axon with radius a = 10μm, $T(a)$ = 80μK and linear expansion coefficient $\alpha = 7 \cdot 10^{-4}$ K^{-1} that is equal to one for polymers [19]. The force value in (8) is $F_{h1} \approx 2.7 \cdot 10^{-11}$ N. In another assumption, using membrane thickens h instead of h_1 in (8), we get affecting force value $F_h \approx 2.7 \cdot 10^{-12}$ N

Thermal processes inside axon

The force influence inside axon body in radial direction should be determined by heat flux from the heated surface area (h_1) to the cylinder axis where $r = 0$. The heat equation [13] in cylindrical coordinates is:

$$\frac{\partial T}{\partial t} = \chi \left(\frac{\partial^2 T}{\partial r^2} + \frac{1}{r} \frac{\partial T}{\partial r} \right) \tag{9}$$

The temperature is $T(r)$, t is a time, radius inside axon is in interval $0 \le r \le a$. The boundary equations are:

$$\begin{aligned} T\big|_{r=a} &= T_{h1} \\ T\big|_{r=0} &< \infty \end{aligned} \tag{10}$$

The process for heating or cooling of the cylinder has a form:

$$T_i = \exp\left(-\chi k_r^2 t\right) \cdot f\{T(r)\}$$

Solution for heat equation in the cylinder is:

$$T = \sum_{n=1}^{\infty} A_n \cdot J_0(k_{r,n} r) \cdot \exp\left(-\chi k_{r,n}^2 t\right) \tag{11}$$

The coefficients in (11) have a form:

$$A_n = \frac{2}{a^2 J_1^2(k_{r,n} a)} \int_0^a r f(r) J_0(k_{r,n} r) dr \tag{12}$$

The final solution is:

$$T(r,t) = \frac{2}{a^2} \sum_{n=1}^{\infty} e^{-\chi k_{r,n}^2 t} \frac{J_0(k_{r,n} r)}{J_1^2(k_{r,n} a)} \cdot \int_0^a r f(r) J_0(k_{r,n} r) dr \tag{13}$$

We put here the constant as a temperature in the heated axon membrane:

$$f(r) = T_{h1} = const \tag{14}$$

The result temperature is

$$T(r) = 2\left(\ T_i / a \ \right) \cdot \sum_{n=1}^{\infty} e^{-\chi k_{r,n}^2 t} \cdot \frac{J_0(k_{r,n} r)}{k_{r,n} \cdot J_1(k_{r,n} a)} \tag{15}$$

This temperature (14) could be further approximated as one summand in a series in approximation of the heating processes in Hodgkin – Huxley model equation [21, 22], and solution should be calculated from (13) with $f(r,t)$.

Comparison the terms with $n = 1$ and $n = 2$ of the simplest case solution (15) is here below. The first and second arguments of the Bessel function have numbers at axon boundary:

$$(k_{r,1})^2 = 2.41^2 / a^2 = 5.76 \cdot 10^{10} \text{ m}^{-2};$$

but $(k_{r,2})^2 = 5.52^2 / a^2 = 5.52^2 \cdot 10^{10}$ m^{-2}`$= 30.5 \cdot 10^{10}$ m^{-2}.

An example heating time in experiments is $t \approx 1$ ms hence $\chi t \approx 10^{-10}$ m^2. Then example axon radius is $a = 10$ μm, so $a^{-2} = 10^{10}$ m^2. We obtain decrement factors for the first and second terms in (15) in the form of the next rapidly decreasing values:

$$A_1 = \frac{1}{\exp\left(\chi t k_{r1}^2\right)} = 1 / \exp\left(2.41^2\right) \approx 3.00 \cdot 10^{-3} \tag{16}$$

$$A_2 = 1 / \exp\left(5.52^2\right) \approx 5.8 \cdot 10^{-14}$$

Since the amplitude of the second harmonic is much smaller than the first harmonic, the temperature in the formula (15) could have only one term, we obtain the final solution:

$$T(r) \approx 2T_{h1} \cdot \frac{\exp\left(-\chi t k_{r1}^2\right)}{a k_{r,1}} \cdot \frac{J_0(k_{r,1} r)}{J_1(k_{r,1} a)} \tag{17}$$

Let's compare the temperature (17) near the surface ($r \approx a$) in the vicinity of the axon axis $r = 0$. The Bessel function argument tends to zero then $r \approx 0$, so temperature in (17) has a factor:

$$\left| \ J_0(0) \ \right| \approx 1 - \frac{(k_{r1} a)^2}{4} + \ldots \approx 1 \tag{18}$$

The argument of J_0 function near cylindrical surface is $k_{r,1} a = 2.41$ (5). Bessel function transforms to (19) [14] then we consider that argument is large, so we get the next factor for (17):

$$\left| \ J_0\left(k_{r,1} a\right) \ \right| \approx \sqrt{\frac{2}{\pi k_{r,1} a}} \cos\left(k_{r,1} a - \frac{\pi}{4}\right) \approx 0.028 \tag{19}$$

From these estimates (17-19) we can see that the amplitude of the temperature on the axis of the cylinder many times exceeds the surface temperature:

$$\left|\mathrm{T}(0)\right| / \mathrm{T}(a) \sim 1 / 0.028 \approx 36 \tag{20}$$

As proved, heat concentration on the axon-cylinder axis can cause the excitation of longitudinal vibrations of the

neurons; it is a direct result of heating during nervous signal propagation.

To evaluate the heat losses in the outer region of the axon, let's consider the temperature distribution in the radial direction far from the cylinder surface then $a<r<\infty$. In the external medium for a cylinder the principle of radial temperature decrease is described by modified Bessel function $K(k_{r,1}a)$. The same argument from (19) ($k_{r,1}a$) >> 1), but $K(k_{r,1}a)$ describes the field outside the axon:

$$K_0(k_r r) \approx \sqrt{\frac{\pi}{2(k_r r)}} \exp(-k_r r) \tag{21}$$

Unknown field coefficient Cons_0 could be finding from the equality of temperatures on the boundary functions inside (17) and outside (21) of the cylinder by the ratio:

$$T(k_r a) \approx Cons_0 \cdot K_0(k_r a) \tag{22}$$

$$T_{h1} \approx \text{Cons}_0 \cdot \sqrt{\frac{\pi}{2k_{r1}a}} \exp(-k_{r1}a)$$

$$Cons_0 \approx \frac{T_{h1}}{\exp(-k_{r1}a)} \sqrt{\frac{2(k_{r1}a)}{\pi}} \tag{23}$$

For argument $k_{r,1}a$ = 2,41 we get $|\text{Cons}_0| \approx 10^{-3}$. Let's assume that during the time (t) the heat wave reaches the axis of the cylinder ($a \sim \sqrt{\chi t}$), but the heat wave goes to the same distance far from the cylindrical surface, so considered outside distance is $a < r < 2a$.

The thermal energy is the function of the temperature T, $E = C_p \rho L S \Delta T$, where C_p is specific heat capacity, but S is the inside heated cross-section $S_a = \pi a^2$, or outside one $S_{2a} = \pi\{(2a)^2 - a^2$. The ratio ($\Delta E$) for the lost and useful heating is equal to the ration of outside energy to inside one, for mentioned numerals it can be estimated as follow:

$$\Delta E = \frac{T_{out} \cdot S_{2a}}{T_{in} S_a} \tag{24}$$

$$T_{out} = Cons_0 \int_a^{2a} K_0\left(\frac{2.41}{a} r\right) dr \tag{25}$$

$$T_{out} \approx Cons_0 \int_a^{2a} \sqrt{\frac{\pi}{2r} \cdot \frac{a}{(k_{r1}a)}} \exp\left(-\frac{2.41}{a} r\right) dr \tag{26}$$

$$T_{in} = \left\{ \frac{2\exp(-\chi t k_{r1}^2)}{(a k_{r1}) J_1(k_{r1}a)} \int_0^a J_0\left(\frac{2.41}{a} r\right) dr \right\} \tag{27}$$

The result in (24) with- (25-27) is about 2% of energy losses for considered axon parameters. Estimates have shown small loss of heat into the outer region of the axon; that is almost all energy will go on heating of the axon with concentration in axis. For the most accurate solution the heating process may be represented as a series of consecutive time-points with appropriate series of constant temperatures T_{h1} on the surface in accordance with variable ions current in membrane. The resulting heat flow will be determined by appropriate series; approximation of Hodgkin - Huxley model described in science literature [21-22] and etc.

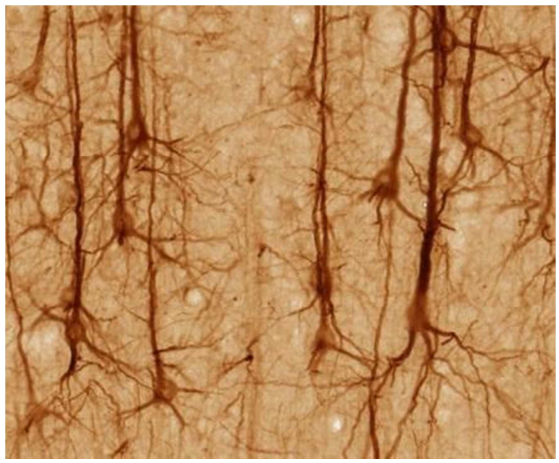

Figure 1a. *The photo of neurons, SMI32-stained pyramidal neurons in cerebral cortex [20].*

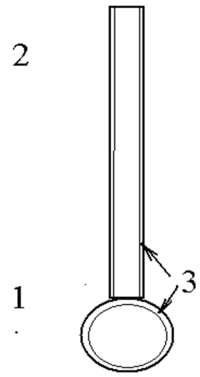

Figure 1b. *Neuron scheme: 1 is the Soma, 2 –axon, 3 - membrane.*

Longitudinal macro-vibration analysis for the axon

The concentration of heat on the cylinder axis probably leads to a longitudinal vibration, because the greatest thermal expansion of the material will be at cylinder axis with the same energy concentration along the axis. This effect can cause the longitudinal vibrations of the axon that may explain the macro reduction observed in practice regularly. The frequency and amplitude of these reductions can be calculated on the basis of this analysis. Longitudinal vibrations [15] of a beam with a cylindrical cross section are described by equation

$$SE \frac{\partial^2 U}{\partial z^2} - \rho S \frac{\partial^2 U}{\partial t^2} = 0 \tag{28}$$

Let's introduce the dimensionless coordinate $\eta = z/L$. The initial and boundary conditions are:

$$U(\eta, 0)\big|_{t=0} = 0 \tag{29}$$

$$U(0, t)\big|_{\eta=0} = 0 \tag{30}$$

The result solution of (28-30) is:

$$U(\eta,t) = Cons_1 \cdot \sin(\eta)\sin(\omega t) \tag{31}$$

The frequency equation from (28-31) is:

$$\frac{E}{\rho L^2} - \omega^2 = 0 \tag{32}$$

The resonance frequency for this kind of vibration formula is:

$$\omega_0^2 = \frac{C^2}{L^2} \ , \quad f_0 = \frac{C}{2\pi L} \tag{33}$$

3. Results and Discussions

The calculations are presented in Table 1 for several console's sizes in the range of real neurons sizes.

Table 1. *The resonance frequency (33) of the longitudinal vibration for axon length L with account of sound velocity C = 192 m/sec.*

305.6	**611.2**	**3056**	**6112**	**30558**	f_0, **Hz**
100	50	10	5	1	L, mm

Vibration equation taking into account the coefficient of the surrounding friction, μ, and exited force in right side, has a form:

$$SE\frac{\partial^2 U}{\partial z^2} - \mu\frac{\partial U}{\partial t} - \rho S\frac{\partial^2 U}{\partial t^2} = F \tag{34}$$

Here $S = \pi r^2$ is axon cross section, E is a Young's modulus, ρ is a density material, wherein the sound velocity is known and presented as $C^2 = E/\rho$. Appropriate uniform equation is:

$$\frac{C^2}{L^2}\frac{\partial^2 U}{\partial \eta^2} - \frac{\mu}{\pi r^2 \rho}\frac{\partial U}{\partial t} - \frac{\partial^2 U}{\partial t^2} = 0 \tag{35}$$

The circular frequency for the equation with attenuation in environment is presented in the form:

$$\omega_1^2 \approx \frac{C^2}{L^2} - \left(\frac{\mu}{2\pi r^2 \rho}\right)^2 \tag{36}$$

Then $\omega_1 < \omega_0$, the resonance frequency [15] formula is:

$$f_1 \approx \frac{C}{2\pi L}\left[1 - \left(\frac{\mu}{2\pi\rho r^2}\frac{L}{C}\right)^2\right]^{0.5} \tag{37}$$

The second option is too high influence of the environment then additional term μ/(2πρr2)> ω0 exceeds initial resonant frequency in a vacuum. Oscillation can not be continued and marked further as '*i*' that is imaginary. In this second case, the oscillations tend from the limitation to the batch due to very strong attenuation. A series of frequency calculations in viscous media were done by the formula (35), the results are shown in Table 2.

Table 2. *The resonance frequency f_1 (37) for cylinders inside water with its viscosity $\mu = 1 \cdot 10^{-3}$ Pa·s.*

r= 10 μm, f_1**, Hz**	**r= 5 μm,** f_1**, Hz**	**r=1μm,** f_1**, Hz**	**L mm / f Hz**
30557	30541	17092	1 mm
6106	6027	-i	5 mm
3045	2883	-i	10 mm
556	-i	-i	50 mm
171	-i	-i	100 mm

Evaluation of the frequency shifts *df* are caused by changes in viscosity and density in the environment; that is calculated using the formula $df = f_0 - f_1$. These calculations are presented in Table 3 for two axon sizes:

A- L = 1 mm with r = 5 μm;

B - L = 10 mm with r = 10 μm.

The air viscosity is $\mu = 1.8 \cdot 10^{-5}$ Pa·s, but the olive oil has $\mu = 43.2 \cdot 10^{-3}$ Pa·s, and intermediate mixture were considered at Table 3.

Table 3. *Resonant frequency (f_1) and its shift (df) for different medium viscosity μ, for two axons A, B.*

f_1 **Hz B**	*df* **Hz A**	f_1 **Hz A**	**μ, Pa·s**
3056	0.005	30558	$1.8 \cdot 10^{-5}$
3045	17	30541	10^{-3}
2960	152	30406	$3 \cdot 10^{-3}$
1709	1729	28829	$10 \cdot 10^{-3}$
-	7686	22872	$20 \cdot 10^{-3}$
-	27422	3136	$30 \cdot 10^{-3}$
-	-	-	$43 \cdot 10^{-3}$

Longitudinal vibrations in the water in the most cases exist; where the frequency is not the imaginary value from the formula (36). Above calculations show a strong dependence of the resonance frequency to medium viscosity for the longitudinal vibrations. The frequency shift in the air relative to vacuum is negligible small. The frequency shift of the vibration in the water is large enough to determine appropriate small changes in viscosity. Calculations show the df = 0.34 Hz for the first axon A (L = 1 mm, r = 5 μm) due to 1-percent change of water viscosity up to $\mu = 1.01 \cdot 10^{-3}$ Pa·s. The second axon B (L = 10 mm, r = 10 μm) shows frequency change the df = 0.34 Hz for the same 1% of viscosity change; it should be noted that these frequency shifts can be measured technically easy. Vibrations in olive oil can not exist in most cases. Doctors know the fact of complete anesthesia for nerves in olive oil and similar media.

The resonance frequency shifts according to fluid density changes are negligible small values for longitudinal vibrations; it was confirmed by calculations here for different axon sizes. Considered *df* was calculated depending on the medium density changes $d\rho$ which is varied from ρ = 1 g / cm^3 up to 2 g / cm^3 in the water with a viscosity $\mu = 1.0 \cdot 10^{-3}$ Pa·s. Dimensions of investigated axons and their resonance frequencies are:

f_1 = 30540.63 Hz then dρ / ρ = 1 ÷ 2. (Axon L = 1 mm, r = 5 μm);

f_1 = 3045.05 Hz then dρ / ρ = 1 ÷ 2. (Axon L = 10 mm, r = 10 μm);

f_1 = 167.11 then dρ / ρ= 1 ÷ 2. (Axon L = 100 mm, r = 10

μm).

If you change the density of the medium in a wide range, as expected, the resonance frequencies of longitudinal vibrations are practically unchanged.

As a result, calculations show the high sensitivity of the axon vibrations to minor changes in surrounding viscosity. This effect can cause the anesthetic phenomenon, which will be shown in details here in a next section.

Possible transfer of vibration excitation between neuron's parts

Let's consider the body of the nerve cell as a ball due to the comparison of photo and scheme at Figure 1a, b. According to presented mechanical model for propagation of the nerve impulse, we assume here that the vibration of axon causes the vibration of clamped ball (Soma) in the case of their resonance frequencies coincidence. The zero-order Soma vibration will be a sphere pulsations, it increases and decreases the radius periodically evenly around undisturbed position. For high-order vibrations of the ball, it is a wave-like change in ball surface and described by the angle factor: $cos(n\varphi)$, n = 0,1,2,3... Higher vibration mode with n = 3,4,5... can also be exited in practice but rarely, they require a greater excitation energy. The circular resonant frequencies $_R$ of oscillations of the ball in the air are described by the formula [23]

$$\omega_R^2 = n(n-1)(n+2)\frac{T_1}{\rho \cdot R^3} \quad , n = 2,3...$$

$$f_R = \frac{1}{2\pi}\sqrt{n(n-1)(n+2)\frac{T_1}{\rho}R^{-3}} \qquad (38)$$

For a water ball in air with radius R the T_1 is equal to 74 in CGC, [23]. The lowest is n = 2 for pulsation mode, but resonant frequency is:

$$f_R = 1.369\sqrt{n(n-1)(n+2)R^{-3}} \approx 3.87R^{-3/2} \qquad (39)$$

In real biology all neurons are placed in water medium. Let's consider liquid ball (ρ = 1.05 g/cm^3) inside liquid surrounding with ρ_1= 1.0 g/cm^3; the resonance frequencies then n≥2 are:

$$f_{Rw} = \frac{1}{2\pi}\sqrt{n(n+1)(n-1)(n+2)\frac{T_1}{\left[(n+1)\rho + n\rho_1\right]}R^{-3}} \qquad (40)$$

The process of vibration transfer from axon-cylinder to the clamped ball will occur with high efficiency when resonance frequencies for both parts have coincidence. So, we took the axon frequencies from Table 2 and equation (37) to find the ball radius from equation (40) then $f_{Rw} = f_1$, result is the next equation:

$$R_n = \left[n(n-1)(n+1)(n+2)\frac{T_1}{\left[(n+1)\rho + n\rho_1\right]}\right]^{1/3}(2\pi)^{-2/3} f_1^{-2/3} \qquad (41)$$

Not only fundamental mode (n=2) of vibration in a ball could be realized by pushing from vibrated cylinder, in the case of such excitation of higher modes (n=3 or n=4) the appropriate ball radii was found from eq. (41) and presented in Table 4. Calculated ball's radius is R_0 then n = 2, the R_1 is then n = 3, R_2 is then n = 4; results are presented at Table 4. There are axons with sizes:

A- L = 1 mm, r = 5 μm;

B - L = 10 mm, r = 10 μm;

C - L = 50 mm, r = 10 μm;

Table 4. *Appropriate sphere radius R_n (41) to have coincidence for resonance frequency with axon.*

C	B	A	Axon size
556	3045	30541	joint f_1, Hz
304	98	21 μm	R_0, μm
766	150	32	R_1, μm
618	198 μm	43	R_2, μm

The lowest radius values (R_0) seems more believable, because low-mode needs less excitation energy for its realization. The data of Table 4 show that radius of the cell body exceeds the axon radius by the factors:

$$R_0 / r \approx 21\ \mu m / 5\ \mu m \approx 4,$$

for A

axon L = 1 mm, r = 5 μm; (42a)

$$R_0 / r \approx 98\ \mu m / 10\ \mu m \approx 10,$$

for B

axon L = 10 mm, r = 10 μm (42b)

$$R_0 / r \approx 304\ \mu m / 10\ \mu m \approx 30,$$

for C

axon L = 50 mm, r = 10 μm (42c)

Comparison of received proportions in (41a-c) with ones at photo of Figure 1a confirms the presented approach and analysis. Note, that in all cases the sum of side surface for cylindrical axon exceeds this surface of appropriate Soma, so the Stock's friction will have more values for cylinder to provide great frequency change in addition to (37).

New hypothesis for anesthesia mechanism

The anesthetic and other admixtures perform the change the composition of the surrounding fluid around neuron with appropriate response of neurons [24-26]. This paper model consider axon as a cylindrical beam profile which is attached to the cell body (Soma) with larger diameter; both cell's part have different formulas for resonant frequencies and their trends. The axon has a form of long cylinder; it has a possibility of longitudinal vibration which excites due to high axis heating with appropriate material thermal expansion. The longitudinal vibration of the cylinders are very sensitive to the viscosity changes in surrounding in many technique cases. We calculated typical changes in resonance frequencies for axon, they have enough difference due to the

1% in viscosity change to be measured in experiments. The resonance frequencies for axons were calculated (37) for Table 3 depending on viscosity of medium. Calculated radius of Some on the based on common frequency approach (41) was compared with neuron photos at Figure 1a to show the coincidence and justice. The Soma resonance frequency can be calculated by other equation (40) for data at Table 4, the f_{Rw} has no high sensitivity to surrounding. The mentioned aspects can explain the anesthetic influence to stop the signal transfer inside neuron, let's consider the model. We suppose the initial natural tandem and equality of resonance frequencies for both parts as axon and its cell body (Soma). Vibration in axon causes vibration and/or deformation in membrane of Soma with membrane ion current as a result signal. This vibration transfers have high efficiency only in the case of resonance coincidence for both parts of neuron. A similar effect has a musical tuning fork, then blow inside one part leads to vibration of adjacent part, and both have the same resonance frequencies due to their similar size there. Our model calculations demonstrate the different values of frequency shifts for axon and for Soma due to changes in environmental biological liquid. We suppose that nature grow each pair of axon+Soma inside one neuron, their resonance frequency of vibrations are equal to each other in natural area, and n^{th} of the possible natural frequencies of oscillation of the axon coincides with one for Soma.

The anesthesia performer the change in surrounding that brings change in viscosity. This mechanical algorithm can explain the effect of no transfer for signal from far axon terminal up to the Soma then anesthetic admixture was introduced. Therefore, when the vibration is coming from axon to Soma on another frequency, then 'head does not understand and can't move'. So the Soma membrane of the nerve can't vibrate due to its pushing not at common resonance frequency, and result current can not appear inside no deformed membrane of Soma. Presented mechanical approach and presented mathematical calculations need more detailed calculations, analysis and experiments that we hope will be done during further development. However, presented algorithm can serve as a background for further development.

4. Conclusions

Presented calculations show possible acoustic mechanisms for signal transfer from far axon terminal up to cell body (Soma) inside the neurons. The waveguide approach was analyzed with frequencies 5 - 15 MHz for fast signal transfer from local surface deformation. The thermal flow was calculated; the numerals for acted forces and temperature distribution were estimated inside axons. The energy losses into outside region far from axon/cylinder is calculated ≈ 2%, so the most part of received energy after Hodgkin – Huxley membrane capacitor discharge was spend to the useful processes of signal propagation inside neuron.

The highest axial temperature can cause also the low-frequency (0.1 - 10 kHz) longitudinal vibrations inside axon. These amplitudes and resonant frequency shifts were calculated depending on viscosity and density of surrounding liquids near axon (cylinder) and Soma (ball). Presented model and calculated numerals can explain the effect of anesthesia then small admixture of anesthetic into liquid near neuron causes different resonance shifts for axon and Soma with no signal transfer as a result.

Acknowledgment

The authors thanks to Professors Martin Bier and Alexander Murashov from the East Carolina University for their useful discussions in the theme.

References

[1] Hodgkin, A. L.; A. F. Huxley, "Currents carried by sodium and potassium ions through the membrane of the giant axon of Loligo," J. Physiol. V. 116, pp. 449–472, 1952.

[2] Hodgkin, A. L.; A. F. Huxley, "A quantitative description of membrane current and its application to conduction and excitation in nerve," J. Physiol., V. 117, pp. 500–544, 1952.

[3] Purves D, at all, Ed., "Neuroscience," by Sinauer Associates, Inc. 2004.

[4] Heimburg T. and A. D. Jackson, "On soliton propagation in biomembranes and nerves," PNAS, V. 102, no. 28, pp. 9790-9795, 2005.

[5] Heimburg Thomas, "Physical Properties of Biological Membranes. Chapter for "Encyclopedia of Applied Biophysics," in H. Bohr, Ed. Wiley-VCH, Weinheim, pp. 593-616, 2009.

[6] Kassahun B. T., A. K. Murashov, M. Bier, "A thermodynamic mechanism behind an action potential and behind anesthesia," Biophysical Reviews and Letters Vol. 5, No. 1 pp. 35-41, 2010.

[7] Wu Di and A. K. Murashov, "MicroRNA-431 regulates axon regeneration in mature sensory neurons by targeting the Wnt antagonist Kremen 1," Frontiers in Molecular Neuroscience, V. 6, Article 35, Oct. 2013.

[8] Lacroix J. J., F. V. Campos, L. Frezza, F. Bezanilla, "Molecular Bases for the Asynchronous Activation of Sodium and Potassium Channels Required for Nerve Impulse Generation," Neuron, V. 79, no 4, pp. 651–657, 2013.

[9] Guixue Bu, H. Adams, E. J. Berbari, M. Rubart, "Uniform Action Potential Repolarization within the Sarcolemma of In Situ Ventricular Cardiomyocytes," Biophysical Journal V. 96, pp. 2532–2546, 2009.

[10] Kaufmann, K. "On the role of the phospholipid membrane in free energy coupling," Caruaru, Brazil 1989.

[11] Giering K., Minet O., Lamprecht I., Muller G. "Review of thermal properties of biological tissues," in "Laser induced interstitial thermotherapy" Ed. by Muller G. J., Roggan A. SPIE, pp. 45 – 65. 1995.

[12] Al Martini, Frederic Et., "Anatomy and Physiology" 2007 Ed. 2007 Edition. Rex Bookstore, Inc. p. 288, 2007.

[13] Carslaw H. S., J. C. Jager, "Conduction of heat in solids", Nauka, Moscow, 487p., 1964.

[14] Abranowitz M. and I. S. Stegun, 'Handbook of mathematical function', Nauka, Moscow, 830p., 1979.

[15] Filippov. A. P. "Vibrations of the deformed systems", Mashinostroenie, Moscow, 734p., 1970.

[16] TTulaikova T., S. Amirova, Hannes Bleuler and Philippe Renaud "Optical-Mechanical Method for Measurements in Micro-Technologies," Proc. of SPIE, V. 5553, pp. 338-347, 2004.

[17] Gurchonok G. A., I. A. Djodjua, S. R. Amirova, T. V. Tulaikova., "Using fiber gratings in the short-length sensors based on micromechanical vibrations," Sensors and Actuators V. A93, pp. 197-203, 2001.

[18] Skudrzyk E., "The Foundations of Acoustics: Basic Mathematics and Basic Acoustics," Springer,-Verlag Wien, New York, 1971.

[19] Seip R, P. VanBaren, C. A. Cain, E. S. Ebbini, " Noninvasive real-time multipoint temperature control for ultrasound phased array treatments," IEEE Trans. Ultrason. Ferroelec. Freq. Contr., V. 43, no 6, pp 1063-1073, 1996.

[20] Photo by UC Regents Davis campus (http://brainmaps.org) [CC BY 3.0 (http://creativecommons.org/licenses/by/3.0)], via Wikimedia Commons.

[21] Levenberg, K. "A Method for the Solution of Certain Non-Linear Problems in Least Squares," Quarterly of Applied Mathematics, 2, pp. 164–168, 1944.

[22] *Marquardt, D. W. "An Algorithm for Least-Squares Estimation of Nonlinear Parameters", Journal of the Society for Industrial and Applied Mathematics, V.* 11, *no. 2, pp. 431–440, 1963.*

[23] Lamb H. "Hydrodynamics," part. 2, Moscow, NITZ-press, 2003.

[24] A. D'Ausilio et al. "Grasping synergies: A motor-control approach to the mirror neuron mechanism", Phys. Life Rev. March 2015. DOI: 10.1016/j.plrev.2014.11.002.

[25] M. M. Mariany et al. "Neuronally-directed effects of RXR activation in a mouse model of Alzheimer disaster", Scientific reports 7: 42270, 2017. DOI: 10.1038/srep42270.

[26] G. C. Van de Bittner, "Nasal neuron PET imaging quantifies neuron generation and degeneration", The Jour. Clin. Investig., 2017. https://doi.org/10.1172/JCI89162.